JOURNAL OF NANO AND MATERIALS SCIENCE RESEARCH
Volume 2, No.1 (Maiden edition, 2023), pp. 90-96
Available online at journals.nanotechunn.com/jnmsr

ORIGINAL ARTICLE

Features of spray-made lithium-doped zinc sulphide thin films

P. O. Offor[a,g] , G. M. Whyte[b], F. U. Whyte[a,g], A. D. Omah[a], S. N. Ude[a], C. C. Daniel-Mkpume[a], P. S. Nnamchi[a], C. S. Obayi[a,], I. Y. Suleiman[a], A. C. Nkele[b,d], U. C. Ogbuehi[c], C. P. Ohanu[c], B. A. Okorie[a] and F. I. Ezema[b,e,f,g]*

[a] *Metallurgical and Materials Engineering Department, University of Nigeria, Nsukka, 410001 Nsukka, Nigeria.*
[b] *Department of Physics and Astronomy, University of Nigeria, Nsukka, 410001 Nsukka, Nigeria.*
[c] *Electrical Engineering Department, University of Nigeria, Nsukka, 410001 Nsukka, Nigeria.*
[d] *Colorado State University, Fort Collins, Colorado State, 80523, USA.*
[e] *Nanosciences African Network (NANOAFNET) iThemba LABS-National Research Foundation, 1 Old Faure Road, Somerset West 7129, P.O. Box 722, Somerset West, Western Cape Province, South Africa.*
[f] *UNESCO-UNISA Africa Chair in Nanosciences/Nanotechnology, College of Graduate Studies, University of South Africa (UNISA), Muckleneuk Ridge, P.O. Box 392, Pretoria, South Africa*
[g] *Africa Centre of Excellence for Sustainable Power and Energy Development (ACE-SPED), University of Nigeria, Nsukka.*

KEYWORDS

Spray-made,
Lithium,
Hexagonal
Nanorod-like,
Zinc sulphide

ARTICLE HISTORY

Received: March 25, 2023
Revised: April 24, 2023
Accepted: May 14, 2023

ABSTRACT

The work centered on the features of spray-made Lithium-doped Zinc sulphide (ZnS) thin films. Lithium-doped and undoped ZnS films with 1%, 3% and 5% Lithium concentrations were made. The features of the films were analyzed using X-ray diffraction (XRD), UV-Visible spectroscopy, scanning electron microscopy (SEM), Fourier transform infrared (FTIR), Raman spectrometry, contact angle meter and Photoluminescence (PL) spectroscopy processes. The XRD analysis showed the formation of a hexagonal phase for the samples. SEM showed nanodot-like and nanorod-like nanoparticles. Size of the particles was between 3.707 and 4.614 nm. FTIR exhibited the C=O stretching mode. The energy gap (Eg) ranged from 3.54 to 3.91 eV while the absorption coefficient is between 3.05 × 10^3 and 6.53 × 10^3 cm^{-1} at 3.0 eV. PL showed narrow band edge emission peak at 357 nm. A hydrophilic surface feature was identified. The films find application in optoelectronics and solar cells.

1 Introduction

The greenhouse effect is connected to the existence of carbon dioxide and other pollutants generated by finite conventional energy sources [1]. Clean alternative energy sources are heavily investigated because of increased global energy requirements and the fast depletion of fossil fuel. Nuclear power energy supply is highly restricted because of its dangerous radioactive fission products. The abundant and non-hazardous solar energy source will conveniently supply the energy need of our planet if adequately harnessed. Zinc sulphide (ZnS) is of high potential research interest because it has 3.52 eV energy gap at 300 K and high resistance to photochemical deterioration [2]. It is an inorganic binary substance suitable for use as optical coatings, field effect transistors and solar cells. Its wide band gap lets high energy incident photons to arrive to the window-absorber junction of solar cells which greatly appreciates the blue response of photovoltaic cells [3]. ZnS films have been grown by various thin film synthesizing methods [4, 5]. CSP was adopted in this work due to its simplicity, low cost, scalability, and growth of good quality films.

0 to 10 at.% gallium (y = $[Ga^{3+}]/[Zn^{2+}]$) were used to grow ZnS films by chemical bath deposition (CBD) process [6]. The E_g changed from 3.60 to 3.76 eV. ZnS films doped with nickel were prepared on glass, quartz, and silicon substrates by CBD [7]. PL exhibits a broad band positioned at 430 and narrow band located at 523 nm. Nanoparticles of Mn-doped ZnS were prepared by a liquid-solid-solution route [8]. A strong Mn-

* **CORRESPONDING AUTHORS** | C. S. Obayi, ✉ camillus.obayi@unn.edu.ng

emission band was depicted by 1.0 at% Mn-doped nanoparticles. Undoped and doped ZnS[Cux ZnS(1-x), Mnx ZnS(1-x) and Pbx ZnS(1-x) ($0.2 \leq x \leq 1$)] were fabricated at 275 ℃ via CSP. The optimal efficiency of 1.8 % was realized for the film doped with 10 wt.% of Mn salt solution [9].

Boron doped ZnS films were made at 450 ℃ to 550 ℃ by CSP [10]. Boric acid (H_3BO_3) was used as dopant source. Lead doped zinc sulphide (Zn1-xS:Pbx) films were grown at 275 ℃ via CSP [11]. The transmittance was about 79.21 % which reduced with Pb concentration. The E_g was 3.44 eV for undoped ZnS which appreciated with Pb concentration from 3.46 to 3.68 eV [11]. Undoped and Ag-doped ZnS films were made through CSP [12]. The films were made with 4%, 6%, and 8% silver concentrations. Ag-doped ZnS films were prepared via CSP process [13]. The energy gaps were between 3.11 and 3.60 eV.

This research article considered the impact of 1%, 3% and 5% lithium concentrations on the structural, morphological, and optical features of Li-doped ZnS films made by CSP practice. Besides, FTIR, FT-Raman, contact angle and photoluminescence features were examined. The films were characterized for structural, optical properties, morphological, surface wettability and photoluminescence through the range of techniques including x-ray diffraction, UV-Visible spectroscopy, scanning electron microscopy, Fourier transform infrared, Raman spectrometry, contact angle meter and Photoluminescence spectroscopy processes and the results are discussed. The films were made with 0.1 M $ZnCl_2$, 0.1 M CS $(NH_2)_2$ and 0.001 M, 0.003 M, and 0.005 M concentrations of $Li(NO_3).3H_2O$. Going by the literature checked, this is a fresh work on the making of lithium-doped ZnS films by virtue of the chemical spray pyrolysis (CSP) step.

2 Experimental procedure

Lithium-doped ZnS films were made on glass substrates at 400 ℃ by CSP measure. The substrates were cleaned as outlined earlier [4]. $ZnCl_2$, $CS(NH_2)_2$ and $Li(NO_3).3H_2O$ were used to prepare the spray solution. 0.1 M solution each of $ZnCl_2$ and $CS(NH_2)_2$ was prepared in double distilled water (DDW), and 0.001 M, 0.003 M, and 0.005 M solutions of $Li(NO_3).3H_2O$ in DDW. The spray solution was prepared for 1%, 3%, and 5% Li concentrations, respectively. The samples were tagged as 1%, 3% and 5%. The spray settings used were as outlined earlier [7].

The features of the films were inspected with a Bruker D2 phaser table-top model diffractometer, JEOL JSM-6360 SEM and UV-1800 Shimadzu UV–VIS spectrophotometer, respectively. RAMAN spectra were assessed by Raman Bruker-MultiRAM spectrometer, the FTIR spectra by Perkin Elmer Spectrum One spectrometer, whilst the PL was assessed by Flouromax-4 spectrofluorimeter. The films' thickness was measured with XP Stylus Profiler Instrument howbeit the contact angles and the surface free energy were assessed with contact angle meter.

3 Results and Discussions

3.1 Structural Analysis

The ZnS films' XRD patterns are shown in Figure 1 while their structural parameters are shown in Table 1.

The structural parameters were computed as conveyed previously [5]. The peaks' positions shifted slightly as Lithium concentration increased. Inclusion of Lithium into the ZnS structure was revealed by the 2θ angle shift recorded in Table 1 from 28.969°, 48.544° and 56.323° to 28.975°, 48.563° and 56.350° then to 29.078°, 48.625° and 56.499° as Li concentration increased. The implication is that the peaks of ZnS thin films doped with 1%, 3%, and 5% Li concentrations corresponding to (103), (1011) and (118) planes shifted to higher angle of diffraction as Li concentration increased which is in suitable agreement with [14 - 16]. This further implies that there is inclusion or doping of lithium in the substitutional sites of the hexagonal ZnS matrix as observed in the literature [16].

The interplanar distance decreased as Lithium concentration increased which showed that Li^+ ions with ionic radius 0.060 nm displaced Zn^{2+} ions with ionic radius 0.074 nm in the tetrahedral coordination of hexagonal ZnS matrix. This alteration decreased the distance between both Li–S and Zn–S because the ionic radius of Li^+ ions is lesser than the ionic radius of Zn^{2+} ions as outlined in [14, 15]. The dislocation density and micro strain decreased with crystallite size which also agrees with [14]. All the films have peaks that well-matched JCPDS Card No. 01 – 072 – 0163 hexagonal ZnS structure as depicted in Figure 1.

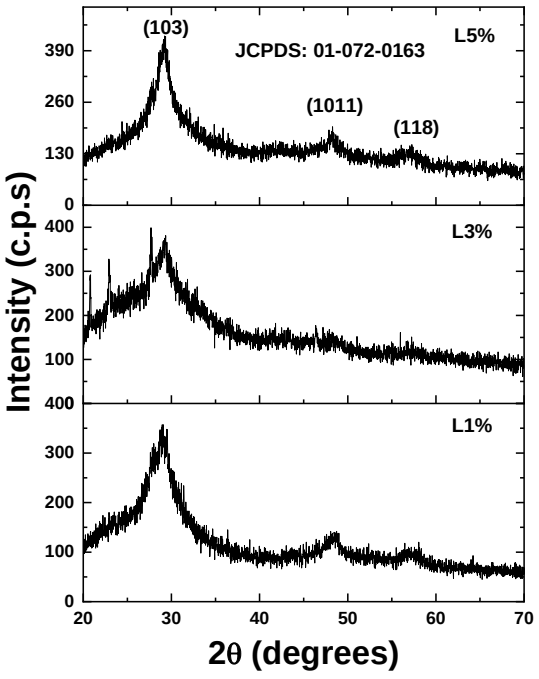

Figure 1: XRD patterns of ZnS films with (a) 1% M, (b) 3% M and (c) 5% M varying lithium concentrations

Table 1: Structural parameters of the films

Sample	Observed 2θ	Standard 2θ	Observed d-spacing (Å)	Standard d-spacing (Å)	FWHM (β in rad)	(hkl)	Crystalline size (G) (nm)	Dislocation density (δ) (Lines/m^2) × 10^{15}	Micro strain (ε) × 10^{-3}
L1%	28.969	29.023	3.080	3.074	0.0579	103	3.707	97.739	31.440
	48.544	48.618	1.874	1.871	0.0281	1011	3.707	97.739	31.440
	56.323	56.441	1.632	1.629	0.0486	118	3.707	97.739	31.440
L3%	28.975	29.023	3.079	3.074	0.0612	103	4.614	81.255	28.954
	48.563	48.618	1.873	1.871	0.0283	1011	4.614	81.255	28.954
	56.350	56.441	1.632	1.629	0.0256	118	4.614	81.255	28.954
L5%	29.078	29.023	3.068	3.074	0.0579	103	4.201	93.249	30.179
	48.625	48.618	1.871	1.871	0.0220	1011	4.201	93.249	30.179
	56.499	56.441	1.627	1.629	0.0490	118	4.201	93.249	30.179

Table 2: FT-Raman frequencies of film with 1% lithium concentration

Wave number (cm^{-1})	Assignment	Wave number (cm^{-1}) [Reference]
246	2 TA	244 [17]
260	Zn-S	261[18]
332	SO mode	334 [19]
377	LA + TO	386, 388 [20], 0-400 [21]
456	LA + LO	454 [21]
480	TO + LA	478 [22]
559	2TO	546, 561 [22]
606	LO+TO	600-700 [19]
782	2LO	778 [22]
854	υ[CC]	841, 844 [18]
955	ρ[CH_2]	932, 918/972, 863 [18]
1086	3LO	1082 [22]
1178	ω[CH_2]	1170, 1171, 1183 [23]

The Raman shift plot and spectral assignments of 1% Li-doped ZnS film are shown in Figure 2 and Table 2, respectively.

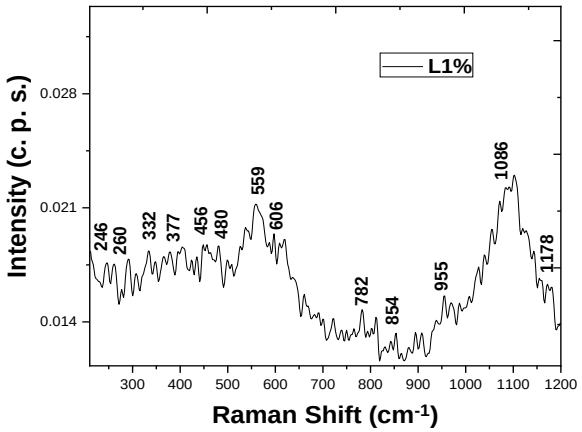

Figure 2: Raman shift of 1% M Li-ZnS thin film

From Table 2, the surface optic (SO) mode is observed at 332 cm^{-1} [19], longitudinal acoustic (LA) and transverse optic (TO) mode are observed [19 - 22]. Zn-S vibration is depicted at about 260 cm^{-1}. Bond stretching υ[CC], bond wagging ω[CH_2] and bond rocking ρ[CH_2] are also displayed.

Moreover, rarely reported first-order (TO and LA), second-order (2TO and 2LO) and third-order (3LO) Raman phonons are revealed. From the Raman spectroscopy, presence of different characteristic bonds of the ZnS thin film is confirmed. These are consistent with those identified with ZnS thin films as displayed in Table 2.

The FTIR plot and spectral assignments of 3% Li-doped ZnS film are shown in Figure 3 and Table 3, respectively.

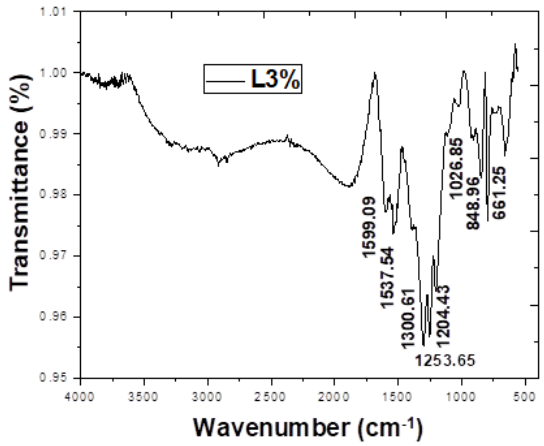

Figure 3: FTIR spectra of 3% M Li-doped film

Chemical bonds present in the deposited thin film are as shown in Table 3. The characteristic major peaks of ZnS can be observed at about 661 and 849 cm^{-1}, which is in conformity with results in references shown in Table 3. C=O stretching mode from atmospheric CO_2 and other bonds contained in the film are provided in Table 3. A number of weak, strong, and broad peaks are available as depicted in Figure 3. This spectrum shows the absorption due to the various Raman vibrational modes.

Table 3: FTIR frequencies of ZnS thin film deposited with 3% lithium concentration

Wave number (cm^{-1})	Assignment	Wave number (cm^{-1}) [Reference]
661	Amides NCN^{2-}	659 [24]
849	Resonance interaction between S^{2-} vibrational modes	851 [25]
1026	C-O stretching mode	1000-1282 [25]
1204	C-O stretching mode	1000-1282 [25]
1254	C-O stretching mode	1000-1282 [25]
1301	C-O stretching + C-H bending	900-1475 [26]
1538	C=O [from CO_2] stretching mode	1500-1650 [27]
1599	C-O stretching mode	1600 [28]

3.2 Surface Morphology

The SEM images of the three films are displayed in Figure 4. The SEM images of the films contained nanodot-like and nanorod-like particles that were unevenly distributed over the surface of the substrates. The nanodot-like particles in the film deposited with 1% M concentration of lithium were closely packed and unevenly arranged on the surface of the substrate. The film deposited with 3% lithium concentration was flower-like nanoclusters and contained cracks whereas the one with 5% lithium concentration was nanodot-like and nanorod-like particles that were unevenly distributed over the surface of the substrates.

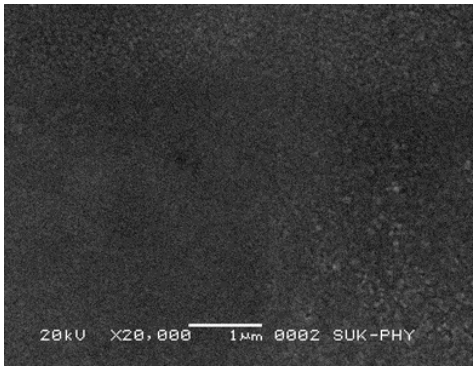

(a)

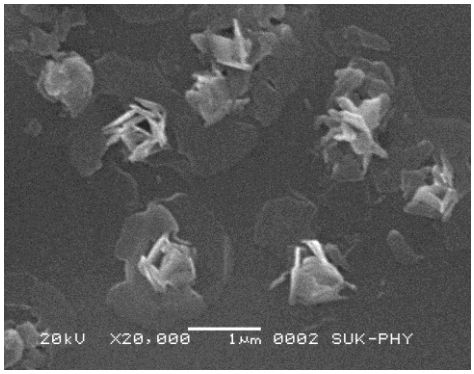

(b)

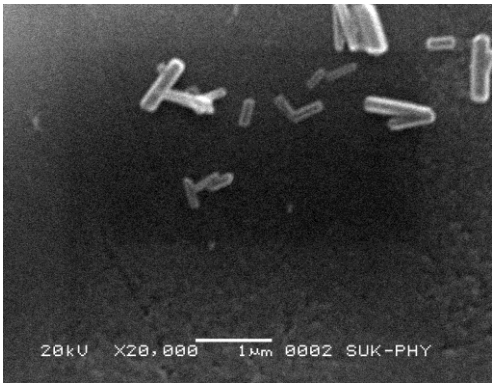

(c)

Figure 4: SEM images of lithium-doped films with (a) 1% M, (b) 3% M and (c) 5% M concentration

3.3 Optical Properties

Figure 5 presents the absorption coefficient of the films. The absorption coefficient was computed as conveyed previously [5]. Figure 5 is a plot of the films' absorption coefficient. The absorption coefficient of the films was 3.05×10^3, 6.53×10^3 and 5.58×10^3 cm^{-1} at 3.0 eV for the films produced with 1%, 3%, and 5% Li concentrations, respectively.

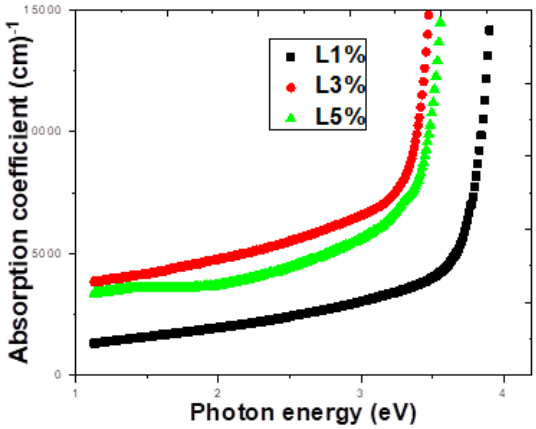

Figure 5: The absorption coefficient of the films

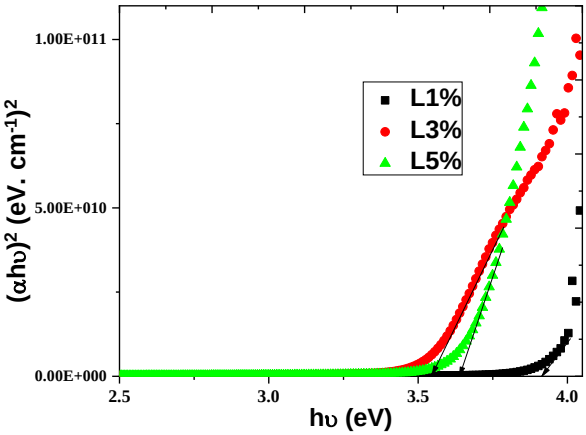

Figure 6: The energy gap (E_g) of the films

Figure 6 presents the energy gaps E_g of the films. The E_g were obtained as conveyed previously [5]. The E_g of the films were 3.91, 3.54 and 3.65 eV for the films produced with 1%, 3%, and 5% Li concentrations, respectively. The E_g are in good harmony with [29, 30]. It has been observed that the structural parameters, thickness, and carrier concentration of thin films affect their E_g [15].

3.3.1 Photoluminescence

PL spectrum of the 3% lithium concentration is shown in Figure 7.

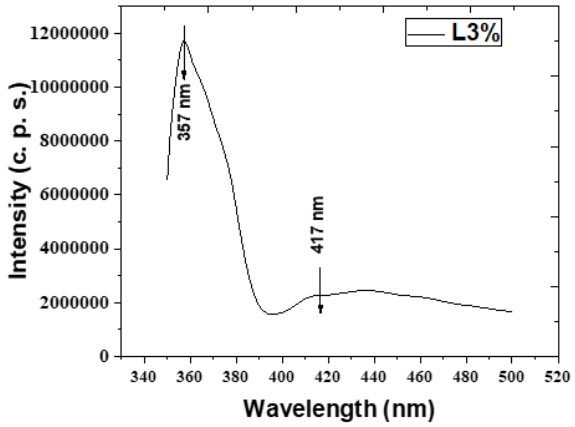

Figure 7: Photoluminescence spectrum of the film with 3% silver concentration

Figure 7 revealed peaks at emission wavelengths of 357 and 417 nm which showed narrow band edge due to mid-band related impurities and presence of Sulphur vacancies due to trapped emissions respectively [30]. The extension of broadened peak may be due to the amorphous glass substrate as given in the literature [31]. The Film's exhibition of photoluminescence at room temperature shows that the film has high optical quality as reported in the literature [32].

3.3.2 Determination of Contact angle

Figure 8 shows the contact angle of the film prepared with 3% lithium concentration.

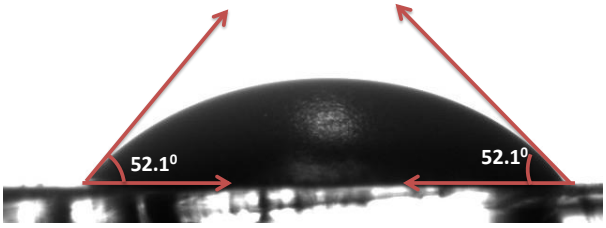

Figure 8: Contact angle of the film with 3% lithium concentration

The wettability behavior of the film is depicted by the value of contact angle, a macroscopic parameter [33]. Figure 8 reveals that the water lies with contact angle of 52.1° on the surface of the ZnS film. This denotes that the surface is hydrophilic in nature. The surface free energy is 52.54 MJ/m^2. The porous structure of the film gave rise to the low water contact angle value that is ascribed to the nanocrystalline nature envisaged to have high surface free energy [33]. The film may enhance the energy storage efficiency of solar cells [13, 30].

4 Conclusion

Good quality spray-made Lithium-doped ZnS films were successfully made by CSP. The films' samples comprised 1%, 3% and 5% lithium concentrations. The films' features were examined by XRD, SEM, FT-Raman, FTIR, PL, spectrophotometer and contact angle meter. The films were of hexagonal structure and the microstructures were nanodot-like and nanorod-like particles. FTIR exhibited the C=O stretching mode. The band gaps lie between 3.54 and 3.91 eV while the absorption coefficient is between 3.05×10^3 and 6.53×10^3 cm^{-1}. PL exhibited band edge emission peak at 357 nm. A hydrophilic surface feature was identified. The films will be suitably useful as window layer for solar cells.

Acknowledgment

The authors hereby appreciate and acknowledge the Africa Centre of Excellence, ACE-SPED, University of Nigeria Nsukka, Nigeria for their kind supports.

Declaration of Competing Interest

Authors have declared that there is no existing conflict of interest.

References

[1] K. Kalyanasundaram (2010), Dye-Sensitive Solar Cells, 1st Ed., EPFL Press, Lausanne, Switzerland, p. 83.

[2] Salim Oudah Mezan, Abdullah Hasan Jabbar, Maytham Qabel Hamzah, Alaa Nihad Tuama, Nabeel Naeem Hasan and Mohd ArifAgam (2018), Synthesis and Characterization of Zinc Sulphide (ZnS) Thin Film Nanoparticle for Optical Properties, Journal of Global Pharma Technology, 10(07) pp. 369-373.

[3] Chelvanathan P., Yusoff Y.F., Haque M., Akhtaruzzaman Alam M. M., Alothman Z.A., Rashid, M. J., Sopian K., Amin N. (2015), Growth and Characterization of RF-Sputtered ZnS Thin Film Deposited at Various Substrate Temperatures for Photovoltaic Application, Applied Surface Science, 334, pp.138–144.

[4] P. O. Offor, B. A. Okorie, F. I. Ezema, V. S. Aigbodion, C. C. Daniel-Mkpume and A. D. Omah (2015): Synthesis and Characterization of Nanocrystalline Zinc Sulphide Thin Films by Chemical Spray Pyrolysis, Journal of Alloys and Compounds, 650, pp. 381 – 385.

[5] Offor P. O., Okorie B. A., Lokhande C. D., Patil P. S., Ezema F. I., Omah A. D., Aigbodion V. S., Ezekoye B. A. and Ezema I. C. (2018): The Properties of Spray-Deposited Zinc Sulphide Thin Films using Trisodium Citrate Complexant, International Journal of Advanced Manufacturing Technology, 95, pp. 1849–1857 http://doi.org/10.1007/s00170-017-1326-6

[6] Abdelhak Jrad, Wafa Naffouti, Tarek Ben Nasr and Najoua Turki-Kamoun (2016), Comprehensive Optical Studies on Ga-Doped ZnS Thin Films Synthesized by Chemical Bath Deposition, Journal of Luminescence, http://dx.doi.org/10.1016/j.jlumin.2016.01.016

[7] Reza Sahraein and Soraya Darafarin (2014), Preparation of Nanocrystalline Ni Doped ZnS Thin Flms by Ammonia-Free Chemical Bath Deposition Method and Optical Properties, Journal of Luminescence, 149, pp. 170–175.

[8] Dongyeon Son, Dae-Ryong Jung, Jongmin Kim, Taeho Moon, Chunjoong Kim, and Byungwoo Park (2007), Synthesis and Photoluminescence of Mn-Doped Zinc Sulfide Nanoparticles, Appl. Phys. Lett. 90, pp. 101910-1 - 101910-3, http://dx.doi.org/10.1063/1.2711709

[9] Mahdi H. Suhail, OmedGh. Abdullah, Raoof A. Ahmed and Shujahadeen B. Aziz (2018), Photovoltaic Properties of Doped Zinc Sulfide/n-Si Heterojunction Thin Films, Int. J. Electrochem. Sci., 13, pp. 1472 – 1483, doi: 10.20964/2018.02.50

[10] Özlem Işildak Ceviz, Yahya Özdemir, Metin Bedir and Mustafa Öztaş (2013), Effect of the Substrate Temperature on the Characterization of Spray-Deposited ZnS:B Films Developed in Science Parks, Journal of Optoelectronics and Biomedical Materials, Vol. 5 Issue 3, July - September 2013 p. 51 – 55.

[11] Mahdi Hasan Suhail and Raoof Ali Ahmed, (2014), Structural, optical and electrical properties of Lead doped zinc sulfide thin films prepared by chemical spray pyrolysis technique, International Journal of Information Technology (IIJIT),Vol. 2, Issue 9, pp. 11 – 17.

[12] Inass Abdulah Zgair, Asmahan Asaad Muhmood, Adel. H. and Omran Alkhayatt (2018), Influence of Ag Dopant Content on Structural and Optical Energy Gap of Zns Thin Films Deposited by Spray Pyrolysis Technique, Transylvanian Review: Vol. XXVI, No. 29, pp. 7809-78015.

[13] Offor P. O., Whyte G. M., Ezekoye V. A., Omah A. D., Ude S. N., Ocheri C., Ezukwoke N., Ezema I. C., Madiba I. G., Okorie B. A., Maaza M., Ezema F. I. (2019), Structural, Morphological and Optical Properties of Spray-Formed Silver-Doped Zinc Sulphide Thin Films, Optik - International Journal for Light and Electron Optics, 185, pp. 519–528, https://doi.org/10.1016/j.ijleo.2019.03.063

[14] Mohamed Salah, Samir Azizi, Abdelwaheb Boukhachem, Chokri Khaldi, Mosbah Amlouk and Jilani Lamloumi (2019), Effects of Lithium Doping on: Microstructure, Morphology, Nanomechanical Properties and Corrosion Behaviour of ZnO Thin Films Grown by Spray Pyrolysis Technique, Journal of Materials Science: Materials in Electronics, Journal of Materials Science: Materials in Electronics, Vol. 30, Iss. 2, pp 1767–1785, https://doi.org/10.1007/s10854-018-0449-3

[15] Mohamed Salah, Samir Azizi1, Abdelwaheb Boukhachem, Chokri Khaldi, Mosbah Amlouk, and Jilani Lamloumi (2017), Structural, Morphological, Optical and Photodetector Properties of Sprayed Li-Doped ZnO Thin Films, J. Mater. Sci., DOI 10.1007/s10853-017-1218-z

[16] Sayanee Majumdar and P. Banerji (2009), Effect of Li Incorporation on the Structural and Optical Properties of ZnO, Superlattices and Microstructures, 45, pp. 583–589, doi:10.1016/j.spmi.2009.03.006

[17] Trajic,´ J., Kostic,´ R., Romcˇevic,´ N., Romcˇevic,´ M., Mitric,´ M., Lazovic,´ V., Balaz,ˇ P., Stojanovic, D. (2015): Raman spectroscopy of ZnS quantum dots, Journal of Alloys and Compounds 637, pp. 401–406.

[18] Kim, S-Y., Hwang, C-S., (2010), Syntheses and Optical Characterizations of ZnS:Mn Nanocrystals Capped by Polyethylene Oxide Molecules of Varying Molecular Weights, Bull. Korean Chem. Soc. Vol. 31, No. 12, pp. 3834 – 3837.

[19] Yung-Tang, N. and In-Gann, C. (2006), Raman Scattering and Electroluminescence of ZnS:Cu,Cl Phosphor Powder, Applied Physics Letters 89, pp. 261906-1 - 261906-3.

[20] Cheng, Y. C., Jin, C. Q., Gao, 1 F., Wu, X. L., Zhong, W., Li, S. H. and Chu, P.K. (2009): Raman scattering study of zinc blende and wurtzite ZnS, Journal of Applied Physics 106, pp. 123505-1 - 123505-5.

[21] Díaz-Reyes, J., Castillo-Ojeda, R., Martínez-Juárez, J., Zaca-Moran, O., Flores-Mena, J. E. and Galván-Arellano, M. (2014),Growth and Characterization of Zns Nanofilms Grown by Rf Magnetron Sputtering on GaAs, International Journal of Circuits, Systems and Signal Processing, 8, pp. 15 – 21.

[22] G¨ode, F. (2011): Annealing Temperature Effect on the Structural, Optical and Electrical Properties of ZnS Thin Films, Physica B 406, pp. 1653–1659.

[23] Kim, J.E., Hwang, C-S., and Yoon, S. (2008), Synthesis and Surface Characterization by Raman Spectroscopy of Water-Dispersible ZnS:Mn Nanocrystals Capped with Mercaptoacetic Acid, Bull. Korean Chem. Soc. 2008, Vol. 29, No. 6, pp. 1247 – 1249.

[24] Rashi, B., Prabin, K.B., Sunandan, B. (2016), Heavy-Metal Ion Sensor Using Chitosan Capped Zns Quantum Dots, Sensors and Actuators, B, 226, pp. 534–539.

[25] Nagamani, K., Revathi, N., Prathap, P., Lingappa, Y., Reddy, K.T.R. (2012), Al-Doped ZnS Layers Synthesized by Solution Growth Method, Current Applied Physics 12, pp. 380-384.

[26] Nagamani, K., Prathap, P., Lingappa, Y., Miles, R. W. and Reddy, K.T. R., (2012): Properties of Al-doped ZnS Films Grown by Chemical Bath Deposition, Physics Procedia, 25, pp. 137 – 142.

[27] Huang, W. H., Chan, S.W., Lee, Y.C. (2015): Optical Properties of Zinc Sulphide Thin Movies Prepared by Spray Pyrolysis, Fabreries Journal, Volume 4, No.2, pp. 35-40.

[28] Ummartyotin, S., Bunnak, N., Juntaro, J., Sain, M. and Manuspiya, H. (2012), Hybrid Organic–Inorganic of ZnS Embedded Pvp Nanocomposite Film for Photoluminescent Application, C. R. Physique 13, pp. 994–1000.

[29] P. E. Agbo, P. A. Nwofe and L. O. Odo (2017), Analysis on Energy Band Gap of Zinc Sulphide (Zns) Thin Films Grown by Solution Growth Technique, Chalcogenide Letters, Vol. 14, No. 8, pp. 357 - 363

[30] P. O. Offor, Assumpta C. Nwanya, A. D. Omah, C. C. Daniel-Mkpume, Malik Maaza, B. A. Okorie, Fabian I. Ezema (2017), Chemical Spray Pyrolysis Deposition of Zinc Sulphide Thin Films using Ethylenediaminetetraacetic Acid Disodium Salt Complexant, Journal of Solid State Electrochemistry, 21:2687–2697, DOI 10.1007/s10008-017-3668-2.

[31] Heine, J.R., Rodriguez-Viejo, J., Bawendi, M.G. and Jensen, K.F. (1998): Synthesis of CdSe Quantum – Dot – ZnS Matrix Thin Films Via Electrospray Organometallic Chemical Vapour Deposition, Journal of Crystal Growth, 195, pp. 564 – 568.

[32] S. M. Pawar, B. S. Pawar, J. H. Kim, Oh-Shim Joo and C. D. Lokhande (2011), Recent status of chemical bath deposited metal chalcogenide and metal oxide thin films, Current Applied Physics 11, pp. 117 – 161

[33] D. S. Dhawale, R. R. Salunkhe, V. S. Jamadade, T. P. Gujar and C. D. Lokhande (2009), An approach towards the growth of polyaniline nanograins by electrochemical route, Applied Surface Science 255, pp. 8213–8216